Article

SOURCE DATA

EMBO reports

Human *Neuralized* is a novel tumour suppressor targeting Wnt/β-catenin signalling in colon cancer

Joo Mi Yi[1,*,†], Tae-Hong Kang[2], Yu Kyeong Han[1], Ha Young Park[3], Ju Hwan Yang[4], Jin-Han Bae[5], Jung-Soo Suh[5], Tae-Jin Kim[5], Joong-Gook Kim[6], Yan-Hong Cui[7,8], Hiromu Suzuki[9], Kohei Kumegawa[10], Sung Joo Kim[11], Yi Zhao[12], In Ja Park[13], Seung-Mo Hong[14], Joon-Yong Chung[15] & Su-Jae Lee[16,*,†]

Abstract

While there is growing evidence that many epigenetically silenced genes in cancer are tumour suppressor candidates, their significance in cancer biology remains unclear. Here, we identify human *Neuralized* (*NEURL*), which acts as a novel tumour suppressor targeting oncogenic Wnt/β-catenin signalling in human cancers. The expression of *NEURL* is epigenetically regulated and markedly suppressed in human colorectal cancer. We, therefore, considered NEURL to be a bona fide tumour suppressor in colorectal cancer and demonstrate that this tumour suppressive function depends on NEURL-mediated oncogenic β-catenin degradation. We find that NEURL acts as an E3 ubiquitin ligase, interacting directly with oncogenic β-catenin, and reducing its cytoplasmic levels in a GSK3β- and β-TrCP-independent manner, indicating that NEURL-β-catenin interactions can lead to a disruption of the canonical Wnt/β-catenin pathway. This study suggests that NEURL is a therapeutic target against human cancers and that it acts by regulating oncogenic Wnt/β-catenin signalling.

Keywords epigenetic alterations; *Neuralized*; tumour suppressor; ubiquitin E3 ligase; Wnt/β-catenin pathway

Subject Categories Cancer; Post-translational Modifications & Proteolysis; Signal Transduction

DOI 10.15252/embr.202256335 | Received 19 October 2022 | Revised 26 May 2023 | Accepted 5 June 2023 | Published online 21 June 2023

EMBO Reports (2023) 24: e56335

Introduction

The Wnt signalling pathway is broadly involved in cell differentiation, embryonic patterning, proliferation and adult homeostasis (Nusse & Clevers, 2017). Genetic mutations in the core components of the Wnt pathway, including adenomatous polyposis coli (APC), axis inhibitor protein 1 (AXIN1) and β-catenin, are well-established causes of aberrant signalling that lead to colon cancer (Clevers, 2004; MacDonald *et al*, 2009). These genetic defects result in the accumulation of β-catenin in the nucleus, followed by association with the T-cell factor (TCF)/lymphocyte enhancer-binding factor (LEF) transcription cofactor family to activate oncogenic target genes, such as *Cyclin D1* and *c-Myc* (He *et al*, 1998; Tetsu & McCormick, 1999). Moreover, there is increasing evidence that aberrant activation of the Wnt/β-catenin signalling pathway is a major driving force for tumorigenesis in various human cancers (Nusse & Clevers, 2017; Bugter *et al*, 2021). Consequently, great effort has been made to understand the targeting of this pathway for the development of therapeutic strategies (Bugter *et al*, 2021; Yu *et al*, 2021).

1 Department of Microbiology and Immunology, College of Medicine, Inje University, Busan, South Korea
2 Department of Biological Science, Dong-A University, Busan, South Korea
3 Department of Pathology, College of Medicine, Inje University, Busan, South Korea
4 Department of Physiology and Convergence Medical Science, Institute of Health Sciences, Gyeongsang National University Medical School, Jinju, South Korea
5 Department of Integrated Biological Science, College of Natural Sciences, Pusan National University, Busan, South Korea
6 Research Center, Dongnam Institute of Radiological and Medical Sciences, Busan, South Korea
7 Department of Life Science, Research Institute for Natural Sciences, Hanyang University, Seoul, South Korea
8 Section of Dermatology, Department of Medicine, University of Chicago, Chicago, IL, USA
9 Department of Molecular Biology, Sapporo Medical University School of Medicine, Sapporo, Japan
10 Cancer Cell Diversity Project, NEXT-Ganken Program, Japanese Foundation for Cancer Research, Tokyo, Japan
11 Department of Pathology, Kyung Hee University Hospital at Gangdong, Kyung Hee University School of Medicine, Seoul, South Korea
12 Institute for Translation Medicine, Qingdao University, Qingdao, China
13 Department of Colon and Rectal Surgery, Asan Medical Center, University of Ulsan College of Medicine, Seoul, South Korea
14 Department of Pathology, Asan Medical Center, University of Ulsan College of Medicine, Seoul, South Korea
15 Molecular Imaging Branch, Center for Cancer Research, National Cancer Institute, National Institutes of Health, Bethesda, MD, USA
16 Fibrosis & Cancer Targeting Biotechnology, Seoul, South Korea
*Corresponding author. Tel: +82 51 890 6734; E-mail: jmyi76@inje.ac.kr
**Corresponding author. Tel: +82 2 2039 2601; E-mail: sjlee@fnctbiotech.com
†These authors contributed equally to this work

In addition to genetic mutations in Wnt/β-catenin pathway components, epigenetic events can also contribute to abnormal activation of this signalling pathway in cancer cells. For example, transcriptional silencing associated with promoter DNA hypermethylation of Wnt inhibitors, such as Secreted Frizzled-Related Proteins (SFRPs), Wnt inhibitory Factor-1 (WIF-1) and DICKKOPF-1 (DKK-1), have been reported in colorectal cancers (Suzuki *et al*, 2002; Aguilera *et al*, 2006). To understand their biological functions, the restoration of Wnt inhibitor expression such as SFRP1/2 was investigated and found their effect in the inhibition of Wnt/β-catenin signalling in colon cancer cells, even in the presence of APC or β-catenin mutations (Suzuki *et al*, 2004). These findings suggest that the epigenetic regulation of the Wnt/β-catenin pathway is a potential therapeutic target in human cancer. Moreover, several studies developed direct targeted inhibitors against the Wnt/β-catenin pathway, based on the following aspects: (i) ligand/receptor-targeted drugs binding to ligands or transmembrane proteins involved in Wnt signalling, (ii) porcupine (PORCN) inhibitors abrogating Wnt secretion and Frizzled (FZD)-dependent signalling, (iii) tankyrase (TNKS) inhibitors antagonizing the Wnt/β-catenin pathway, and (iv) β-catenin inhibitors blocking TCF/LEF-dependent transcription (Chen *et al*, 2009; Huang *et al*, 2009; Katoh, 2017; Katoh & Katoh, 2022).

Neuralized (*NEURL*) was originally identified as a neurogenic gene critical for the regulation of Notch signalling during cell-fate decisions in *Drosophila* neurogenesis (Boulianne *et al*, 1991). *Drosophila* NEURL (dNEURL) contains two neuralized homology repeats (NHR) that are evolutionarily conserved and they each contain a Really Interesting New Gene (RING) domain for E3 ubiquitin ligase function (Deblandre *et al*, 2001; Lai *et al*, 2001; Pavlopoulos *et al*, 2001; Yeh *et al*, 2001). The human homologue of dNEURL is encoded at 10q25.1, which is a region exhibiting frequent loss of heterozygosity in astrocytomas. Furthermore, it has been shown that inactivation of NEURL is associated with the progression of astrocytomas (Nakamura *et al*, 1998). A recent gene expression profile supports the above notion that transcriptional silencing of *NEURL* by promoter hypermethylation is correlated with colon cancer progression (Schuebel *et al*, 2007). While it is well characterized as a core component of the Notch pathway to regulate the internalization and degradation of the Notch ligand via its E3 ligase function (Lai *et al*, 2001; Pavlopoulos *et al*, 2001; Yeh *et al*, 2001), the potential tumour suppressor functions of NEURL in human cancer have been poorly defined.

Numerous studies identify epigenetically silenced genes that are considered tumour suppressor candidates in cancer; however, their biological roles in cancer biology are not always well defined. In this study, we uncover that human *NEURL* acts as a tumour suppressor that is associated with oncogenic Wnt/β-catenin signalling in colorectal cancer.

Results

Human *NEURL* is downregulated by promoter hypermethylation in colorectal cancer

To establish the epigenetic regulation of *NEURL* in colorectal cancer (CRC), we analysed promoter methylation in primary CRC using bisulphite pyrosequencing. Elevated levels of *NEURL* methylation were detected in the primary CRC tumours (27%, 12 of 43). In contrast, levels of *NEURL* methylation were low in normal colonic tissues which suggests that *NEURL* has cancer-specific methylation (Fig 1A). Bisulphite sequencing analysis was conducted to confirm the methylation status in selected tissue specimens (Fig 1B), and the results indicated that the promoter region of *NEURL* is densely methylated in CRC samples when compared with normal tissues. *NEURL* was found to be frequently hypermethylated and lacked transcriptional expression in the TCGA-COAD database (Fig 1C and D) (Cancer Genome Atlas Network, 2012). Using two different profiles from the TCGA-COAD databases, we confirmed a strong correlation between DNA hypermethylation and transcriptional downregulation for *NEURL* in CRC patients ($P = 0.00665$, $R = -0.17$) (Fig 1E). The correlation between hypermethylation and *NEURL* protein expression in adjacent normal colons ($n = 3$) and primary tumour tissues ($n = 3$) harbouring hypermethylated *NEURL* was assessed. The *NEURL* expression levels were found to differ drastically between colon cancer and adjacent normal tissues, suggesting that the regulation of *NEURL* is associated with the hypermethylation of its promoter (Fig 1F).

Promoter hypermethylation of *NEURL* is associated with poor outcomes in CRC patients

Promoter hypermethylation-mediated silencing of classical tumour suppressor genes is implicated in poor clinical outcomes (Suzuki *et al*, 2004; Brock *et al*, 2008; Yi *et al*, 2011). The clinical relevance of *NEURL* in colon tumours was, thus, estimated by analysing a dataset of colon cancer samples from TCGA database. We evaluated the correlation between the *NEURL* methylation status and clinical features of CRC patients. Kaplan–Meier survival analysis of these probes revealed that CRC patients with high levels of *NEURL* methylation were associated with poorer survival rates when compared with those with lower levels of *NEURL* methylation (Fig 1G).

NEURL acts as a tumour suppressor in colon cancer

To investigate the possible role of *NEURL* as a tumour suppressor, we determined whether *NEURL* affects the growth rate of colon cancer cells. Cancer cell lines lacking endogenous *NEURL* (RKO, DLD1 and HCT116) due to promoter hypermethylation exhibited robust suppression in colony-forming abilities upon the overexpression of NEURL by transient transfection (Figs 2A and EV1A). To scrutinize the growth-suppressive properties of NEURL, we established HCT116 cells that stably expressed NEURL. Compared to mock or empty vector controls, NEURL-expressing HCT116 cells showed reduced proliferation efficiencies (Figs 2B and C, and EV1A). Moreover, metastatic properties, such as migration (Fig 2D) and invasion (Fig 2E), were compromised by the restoration of NEURL expression. These tumour-suppressive effects were confirmed in other colon cancer cell lines such as DLD1 and LS174T (Fig EV2A–G), as well. To confirm the tumour-suppressive function of NEURL *in vivo*, we used a mouse xenograft tumour assay. The tumour xenografts were established in 6-week-old female immunodeficient mice via the injection of HCT116 cells stably expressing NEURL along with empty vector controls. Tumour volume was significantly smaller in

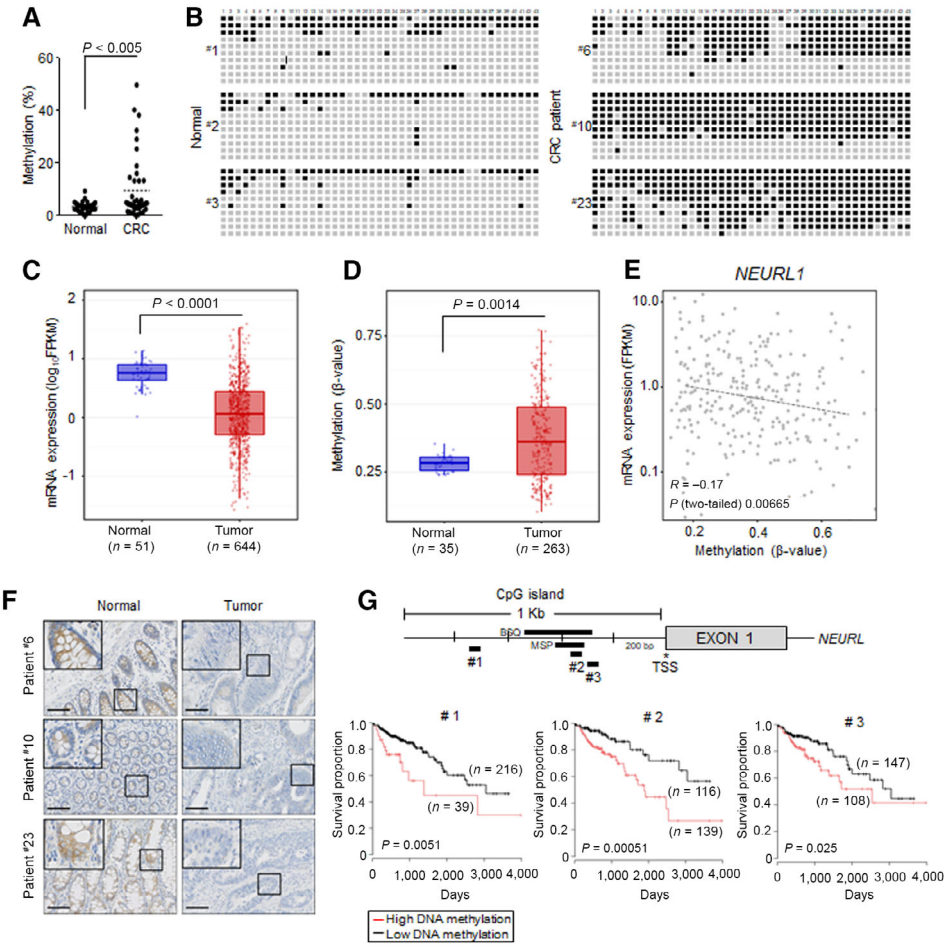

Figure 1. Epigenetic inactivation of human *Neuralized* (*NEURL*) in colon cancer.

A Bisulphite pyrosequencing results for the *NEURL* promoter CpG island in normal colon tissues (n = 34) and primary colorectal cancer tumours (n = 43). The horizontal lines represent the median.

B Bisulphite sequencing analysis of *NEURL* in three representative normal colon tissues and three CRC tumour tissues. Open and filled squares represent unmethylated (u) and methylated (m) CpG sites, respectively, and each row represents a single clone.

C, D Gene expression (C) and promoter methylation (D) profiles for *NEURL* in normal colon and tumour samples from the TCGA-COAD database. Statistical significance was assessed by two-sided Student's t-test.

E Negative correlation between gene expression and promoter methylation of NEURL was observed using the data from TCGA-COAD database (R = −0.17, P = 0.00665).

F Immunohistochemical analysis of NEURL protein expression in normal colon mucosa and CRC tissues. Brown staining represents the NEURL antibody. Each image represents a different patient. Scale bars, 100 μm.

G Kaplan–Meier curves showing the effect of *NEURL* DNA methylation on overall survival among CRC patients (n = 255) from the TCGA-COAD database. Three different probes are located in the CpG islands, in a 1-kb region upstream of TSS (Transcriptional start site; Indicated as asterisk *), which were associated with MSP and BS analyses in this study. Red and black colours indicate individuals with high and low levels of DNA methylation respectively. The schematic representation of the *NEURL* promoter region, including CpG islands, is shown (top). BSQ and MSP indicate the amplification region for bisulphite sequencing and MSP analyses respectively. Numbers (#1, #2, #3) indicate the probe locations from TCGA-COAD methylation database. The results showed that high level of NEURL methylation leads to a worse overall patient survival. (#1); P = 0.051, (#2); P = 0.00051, (#3); P = 0.025. Survival differences between the low DNA methylation NEURL group and the high DNA methylation NEURL group in each set were assessed by the Kaplan–Meier estimate and compared using the log-rank test.

Data information: For (A, C, D), statistical significance was determined by two-sided Student's t-tests; For (C, D), data are presented as box and whiskers plots. The horizontal lines represent the median; the bottom and top of the boxes represent the 25 and 75% percentiles, respectively, and the vertical bars represent the range of the data. For (E), statistical significance was determined by Spearman's correlation test, For (G), statistical significance was performed by log-rank test.
Source data are available online for this figure.

mice injected with HCT116 cells stably expressing NEURL than in those that received control or mock-treated cells (Figs 2F and EV1B). This result was consistent with other colon cancer cell lines, such as LS174T cells overexpressing NEURL by transient transfection (Fig EV2H and I). In contrast, the depletion of endogenous NEURL with shRNA in SW480 cells, which otherwise express NEURL endogenously, showed similar growth rate compared to the control cells *in vitro* (Fig EV2J–L) and *in vivo*. When the tumour volumes reached 100 mm^3, the cisplatin or mitomycin C (MMC) treatment was initiated. Mice received 3 mg/kg of either cisplatin or

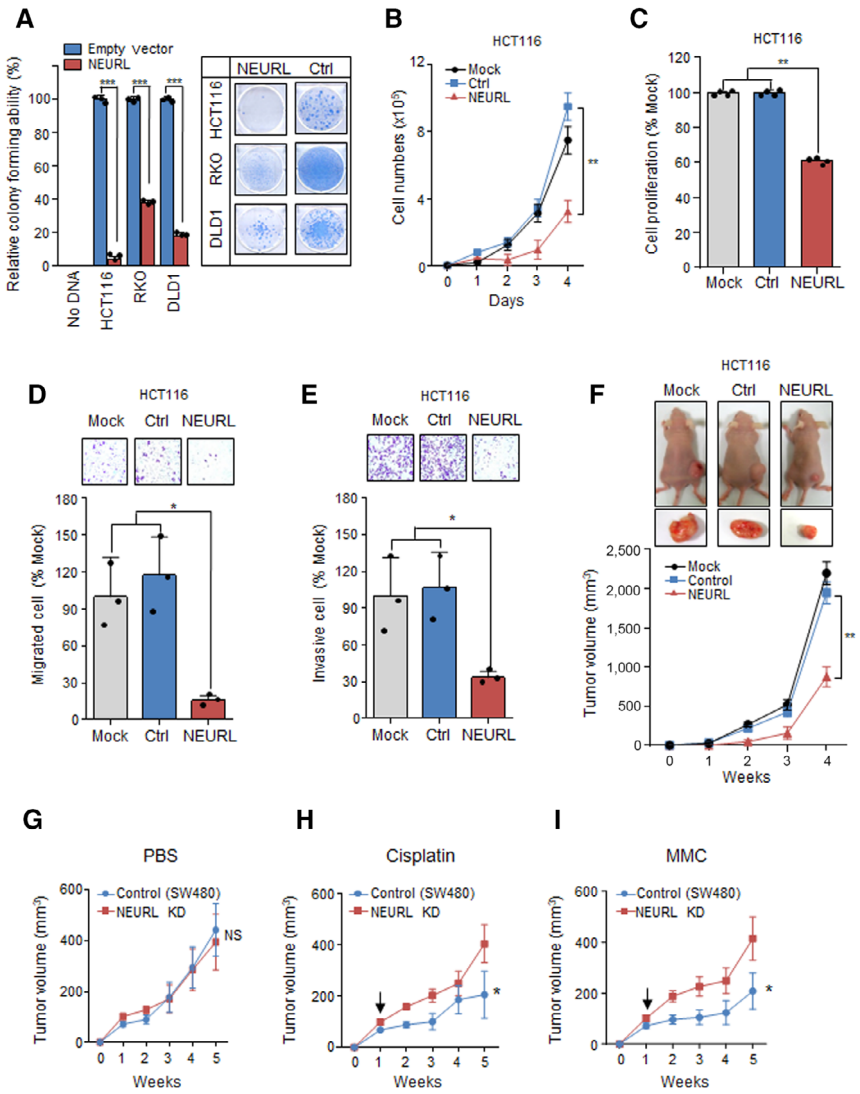

Figure 2. *NEURL* activation has tumour-suppressive effects in colon cancer cells.

A Colony formation assay shows that the ectopic expression of NEURL suppresses HCT116, RKO and DLD1 cell growth. Cells were transfected with a NEURL expression vector or empty vector and then selected with G418 for 12 days. The number of colonies relative to the control is shown on the left. Representative colonies were visualized using light microscopy. Data show mean ± SD. Circles represent biological replicates (n = 3).

B, C The effects of NEURL overexpression on cell proliferation were determined using (B) growth curve and (C) MTT assays. Data show mean ± SD. Circles represent biological replicates (n = 4).

D, E The migration and invasion of mock, empty vector control and NEURL-overexpressing colon cancer cells were evaluated. The bar graphs represent the quantity of (D) migrated cells and (E) invasive cells based on transwell migration and invasion assays respectively. The quantity of the migrated cells represents the mean of three random microscopic fields per membrane. Data show mean ± SD. Circles represent biological replicates n = 3.

F Xenograft assay. Mock, empty vector control or NEURL-overexpressing colon cancer cells were injected subcutaneously into nude mice (n = 14). After 4 weeks, the tumour masses were visualized (top), and the average tumour size was measured at different time points (bottom). Representative photographs of the xenografts (4 weeks) show significant growth suppression with NEURL overexpression relative to the mock and control. Data are represented as the mean ± SD (five mice per group of mock cells and NEURL-overexpressing cells, four mice per group of control cells).

G–I Depletion of NEURL resulted in resistance to chemotherapeutics. SW480 control and KD cells were subcutaneously injected into BALB/c nude mice (n = 42). After 1 week, SW480 tumours were established and then treated with (G) phosphate-buffered saline (PBS) (H) cisplatin, or (I) MMC. At the end of the treatments, mice were sacrificed, and tumours were extracted (bottom right). Data are presented for the guanine (6-tg; 2.5 μg/ml) treatment. Data are represented as the mean ± SD (seven mice per group).

Data Information: For all panels, statistical significance was assessed by two-sided Student's t-tests, data show means ± SD, *Indicates significant differences from control. *P < 0.05, **P < 0.01, ***P < 0.001, NS, not significant. The ectopic or basal expression of NEURL in cell lines we tested in Fig 2 is shown in Fig EV1A–C.
Source data are available online for this figure.

MMC after 7 days of tumour cell injection. Interestingly, the chemotherapeutic treatment significantly suppressed the tumour growth of control SW480-injected mice, whereas NEURL knock-down (KD) tumour-injected mice showed substantial resistance to both drugs (Figs 2G–I and EV1C). These functional data indicate that *NEURL* acts as a tumour suppressor and that the loss of NEURL promotes

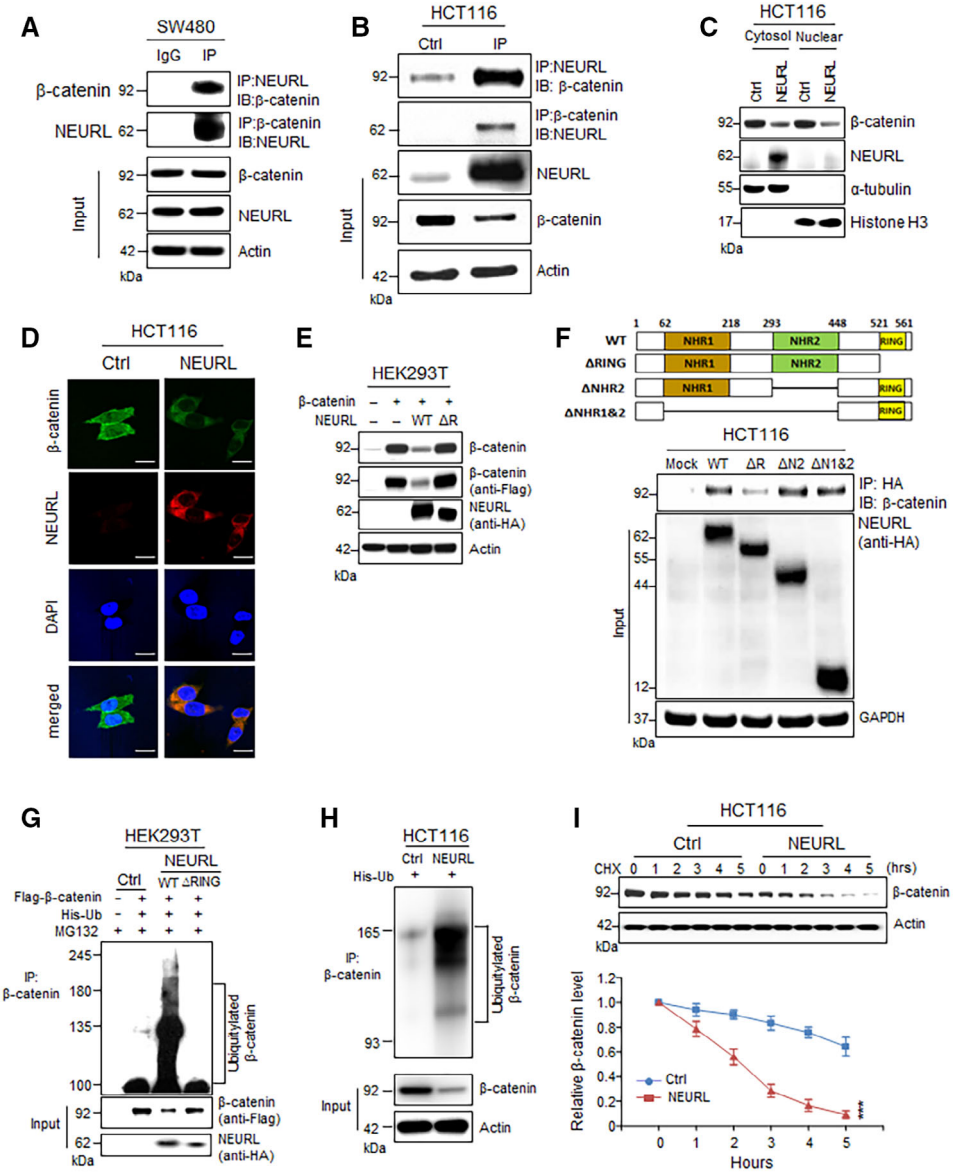

Figure 3.

tumour growth and abrogates the tumour-suppressive effects in colon cancers.

Cytosolic NEURL can interact with β-catenin and promotes its degradation

Two different NEURL isoforms in drosophila have been identified. A plasma membrane-associated ubiquitin ligase that is required for neural development for which Delta internalization is well characterized and is known to be a critical process for Notch signalling (Yeh *et al*, 2000; Lai & Rubin, 2001; Pavlopoulos *et al*, 2001). The other isoform is truncated at the first exon and is predominantly cytoplasmic. Some evidence suggests that mammalian NEURL is localized in the cytoplasm (Timmusk *et al*, 2002; Commisso & Boulianne, 2007), although the functional roles of both NEURL isotypes in Notch signalling in human cancer remain unknown. However, its *Drosophila* homologue is also known as an E3 ubiquitin ligase and E3 ligases can bind β-catenin and contribute to β-catenin degradation during mammalian myogenesis (Nastasi *et al*, 2004).

NEURL protein in colon cancer cell lines (HCT116, RKO, SW480 and Colo320) was found to be predominantly localized to the cytoplasm (Fig EV3A). It was, thus, hypothesized that NEURL may interact with β-catenin through its E3 ligase function, and therefore intersect with the Wnt/β-catenin pathway in colorectal cancer. The Wnt signalling pathway has prominent and widespread roles in development, tissue homeostasis and cancer. A key step in this pathway is the regulation of cytosolic β-catenin levels (MacDonald *et al*, 2009), so it is, thus, reasonable to investigate a potential role for NEURL in the regulation of β-catenin. First, we examined whether NEURL and β-catenin interact at physiological levels using a co-immunoprecipitation (co-IP) assay. Interaction between NEURL

Figure 3. NEURL interacts directly with β-catenin and controls its stability via ubiquitination.

A, B Analyses of the interaction between β-catenin and NEURL. (A) WCLs of SW480 cells were immunoprecipitated with β-catenin or NEURL antibody and subjected to Immunoblot (IB) analyses (B) Co-IP analysis in stably overexpressing NEURL HCT116 cells along with control cells. The input lanes contain 10% of the lysates used in the immunoprecipitation.

C IB analysis for β-catenin levels in the cytosol and nucleus with or without NEURL expression. Cell fractions were prepared from HCT116 cells stably expressing NEURL or empty vectors. Cytosolic fractions and nuclear fractions were probed for β-catenin and NEURL expression. Alpha-tubulin and histone H3 served as loading controls and cell fraction markers.

D Immunofluorescence (IF) analysis of β-catenin levels in the presence and absence of NEURL expression in HCT116 cells. Nuclei were visualized with 4′6-diamidino-2-phenylindole (DAPI, blue). Confocal microscopy was performed. Scale bar, 20 μm.

E β-catenin levels were examined in HEK293T cells transfected with the indicated constructs, cells were harvested and the whole lysates were analysed by immunoblotting. GAPDH was used as a loading control for cell lysates.

F Top panel, Diagram showing the NEURL protein domains, which consist of two neuralized homologous repeat (NHR) domains and a C-terminal RING domain. Bottom panel, HCT116 cells were transfected with the indicated plasmids (HA-tagged) and endogenously expressed high levels of β-catenin. The HA-NEURL protein was immunoprecipitated using an anti-HA antibody. Beta-catenin-bound NEURL protein was detected using an immunoblot with an anti-β-catenin antibody.

G, H NEURL destabilizes β-catenin through ubiquitination. (G) HEK293T and (H) HCT116 (with or without NEURL expression) cells were transfected with the indicated plasmids. Cells were treated with 40 μM MG132 for 3 h prior to lysis and then subjected to anti-β-catenin immunoprecipitation, followed by immunoblotting with the anti-His antibody.

I HCT116 cells stably expressing NEURL or empty vector control cells were incubated with cycloheximide (CHX) for the indicated time points, after which they were collected for IB analysis (top). Quantification of β-catenin was normalized to the loading control and expressed relative to 0 h. Data show mean ± SD (n = 3).

Data Information: For (I), statistical significance was assessed by a two-sided Student's t-test, n = 3, biological replicates; data show mean ± SD, ***P < 0.001. For (D), the ectopic or basal expression of NEURL in HCT116 cells is shown in Fig EV1D.
Source data are available online for this figure.

and β-catenin was detected in NEURL overexpressing HCT116 cells and this interaction was also detected in endogenous NEURL expressing SW480 cells (Fig 3A and B). To understand the physiological relevance of the interaction between NEURL and β-catenin, we investigated the modulation of β-catenin stability by NEURL. The overexpression of NEURL in HCT116 cells could result in a significant decrease in β-catenin levels both in the cytoplasm and nucleus (Figs 3C and D, and EV1D). We also confirmed that when NEURL was transiently transfected to HEK293 cells, they showed a decrease in their β-catenin levels (Fig 3E). However, no significant changes in β-catenin levels were detected when using small interfering RNA (siRNA)-targeted depletion of NEURL in endogenous NEURL-expressing SW480 cells (Fig EV3B).

Human NEURL, similar to its *Drosophila* homologue, consists of three conserved domains: two neuralized homology repeat (NHR) domains and a carboxyl-terminal RING domain. The RING domain is necessary and sufficient for E3 ubiquitin ligase activity (Yeh *et al*, 2000; Lai & Rubin, 2001; Pavlopoulos *et al*, 2001).

By using NEURL deletion mutants, we found that the interaction between NEURL and β-catenin was mediated by the RING domain of NEURL (Fig 3F), indicating that this domain or its ubiquitin ligase activity is required for NEURL-induced β-catenin degradation. In HCT116 cells, we overexpressed NEURL without the RING domain required for interaction with β-catenin, NEURL without other NHR domains and wild-type (WT) NEURL. Endogenous β-catenin levels were decreased by WT NEURL but not by the other mutant proteins (Fig 3F). These results further suggest that its ubiquitin ligase activity is critical for NEURL-induced β-catenin degradation.

To follow up with this finding, we investigated whether NEURL promotes the degradation of β-catenin through ubiquitination. A polyubiquitination assay indicated that WT NEURL increased the ubiquitination of β-catenin in 293T cells, whereas the absent RING domain of NEURL showed no effect (Fig 3G). In agreement with these data, the re-expression of NEURL in HCT116 cells also increased the ubiquitylation of β-catenin when compared with the control (Fig 3H). We confirmed the NEURL-dependent ubiquitylation of β-catenin in denaturing conditions to minimize the contribution of the ubiquitination signal by other potential interactors (Fig EV3C). We also used a cycloheximide (CHX)-based protein chase series to measure the protein stability of β-catenin in HCT116 cells stably overexpressing NEURL. Human NEURL expression enhanced the β-catenin degradation rate (Fig 3I), which suggests that NEURL contributes to β-catenin destabilization in colon cancer cells. Collectively, these results suggest that the restoration of NEURL in colon cancer cells might lead to the suppression of the canonical Wnt signalling pathway through interactions with β-catenin.

Restoration of *NEURL* expression can interrupt the Wnt/β-catenin pathway

The aberrant activation of the Wnt signalling pathway is a prerequisite for tumorigenesis in colon cancer (Clevers & Nusse, 2012). To confirm the biological significance of NEURL in relation to Wnt/β-catenin signalling, T-cell factor/β-catenin transcription assays were conducted to ascertain the transcriptional activity of β-catenin in the context of different transcriptional expression statuses of NEURL (Korinek, 1997). The transcriptional activity of the constitutively active Wnt pathway due to mutated β-catenin was blocked by the overexpression of NEURL in both HCT116 (Ser45 deletion of one β-catenin allele and one WT allele) and LS174T (homozygous activating β-catenin mutation) cells (Figs 4A and B, and EV1D and E respectively). By using the lacking RING domain of NEURL, which destroys its E3 ubiquitin ligase activity, it failed to inhibit β-catenin activity when compared to WT NEURL in HCT116 cells (Figs 4C and EV1D). Moreover, NEURL overexpression significantly inhibited Wnt3a-induced β-catenin transactivation in HCT116 cells and HEK 293T cells (Fig 4C–E respectively).

In addition, the transcriptional activities of both WT β-catenin and the constitutively active β-catenin (S33Y β-catenin) were significantly blocked and reduced, respectively, by the overexpression of NEURL in HEK 293T cells (Figs 4F and G, and EV1F respectively). These data were consistent with the co-staining images showing that the protein level of WT β-catenin and the constitutively active

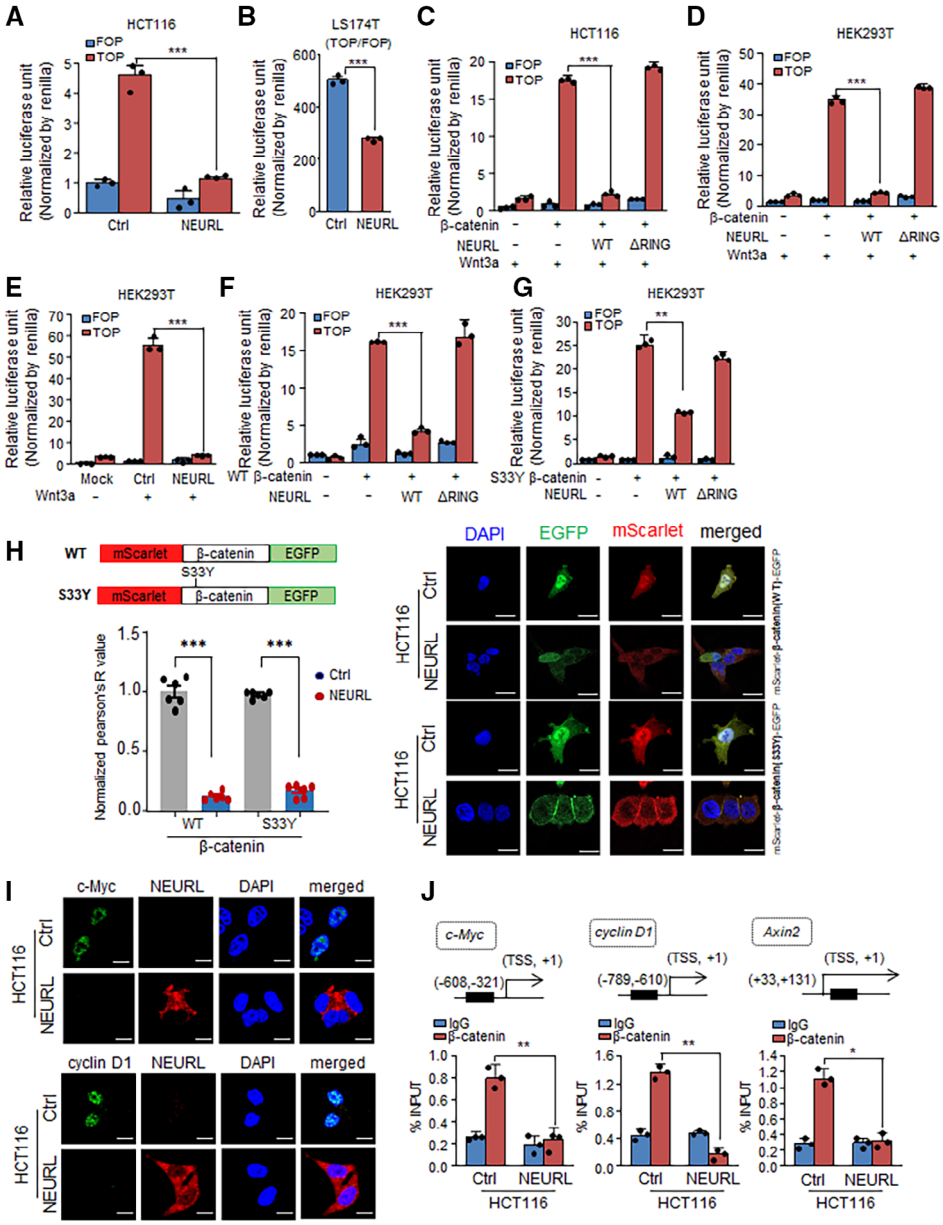

Figure 4.

β-catenin (S33Y) were significantly reduced by the overexpression of NEURL in HCT116 cells by confocal microscopy (Figs 4H, EV1G and EV3D). Taken together, these results demonstrate that NEURL reduced the cytoplasmic β-catenin, leading to inhibition of its transcriptional activity in the nucleus as well as decreasing the overall protein levels of β-catenin.

Furthermore, we investigated whether the functional expression of NEURL resulted in the downregulation of β-catenin target genes, including *c-Myc*, *survivin* and *cyclin D1*, at the mRNA level (Fig EV4A). The results showed that the mRNA levels for 12 target genes including *c-Myc*, *survivin* and *cyclin D1* were significantly downregulated by NEURL expression. In agreement with the mRNA levels of these target genes, marked reductions in the levels of protein were detected in cells stably expressing NEURL when compared with the controls (Fig EV4B). Immunofluorescence analysis confirmed the markedly diminished cellular levels of c-Myc and cyclin D1 in NEURL-expressing cells (Figs 4I and EV1G). Moreover, a chromatin immunoprecipitation (ChIP) assay showed a dramatic decrease in the binding of β-catenin to target promoters in NEURL-expressing cells, and this reduction was augmented by NEURL depletion in control cells (Figs 4J and EV1G). These results strongly suggest that NEURL negatively regulates the β-catenin levels in colon cancer cells.

Interruption of Wnt/β-catenin pathway activity induced by NEURL is GSK3β and β-TrCP independent

To determine whether the downregulation of β-catenin is mediated by the ubiquitin–proteasome pathway, we performed immunoblot analysis in the presence or absence of the proteasome inhibitor

Figure 4. NEURL-β-catenin interactions can interrupt the Wnt/β-catenin pathway.

A, B NEURL regulates the transcriptional activity of β-catenin (A) HCT116 cells stably overexpressing NEURL or control cells and (B) LS174T cells transfected with NEURL WT and control vector were transfected with TOP-Flash with TCF-responsive promoter–reporter or FOP-Flash with non-responsive control reporter, followed by TCF/β-catenin reporter dual-luciferase assay.

C, D Luciferase activity after Wnt3a treatment in (C) HCT116 cells stably overexpressing NEURL and mutants without RING domain or control cells, and (D) HEK293T cells transiently transfected with NEURL and mutants without RING domain or control cells, followed by TCF/β-catenin reporter dual-luciferase assay.

E Luciferase activity of HEK293T cells transfected with the indicated plasmids after Wnt3a treatment. Cells were treated with 20 ng/ml Wnt3a for 6 h, followed by TCF/β-catenin reporter dual-luciferase assay.

F, G Luciferase activity of HEK293T cells was transfected with the indicated plasmids, followed by TCF/β-catenin reporter dual-luciferase assay.

H DAPI, EGFP, mScarlet and merged confocal images in control and NEURL stably expressing HCT116 cells transfected with the WT or S33Y β-catenin constructs. The normalized Pearson's *R* value indicated the co-localized degree of mScarlet and EGFP in the control and NEURL expressing HCT116 cells transfected with the WT or S33Y β-catenin constructs ($n = 6$, $^{***}P < 0.001$).

I IF analysis showing the localization of c-Myc and cyclin D1 in HCT116 cells stably overexpressing NEURL or control cells.

J The TCF-binding region of β-catenin to its promoter of target genes (*c-Myc*, *cyclin D1* and *Auxin*) was assessed using chromatin immunoprecipitation (ChIP), and the target genes were analysed using qRT-PCR between control and NEURL-overexpressed HCT116 cells. ChIP-qPCR analysis for *c-Myc*, *cyclin D1* and *Axin inhibition protein 2* (*Axin2*) for the TCF-binding region of β-catenin.

Data Information: For (A–G), relative TOP/FOP activities depend on NEURL expression. Luciferase activity was measured 48 h after transfection with the dual-luciferase assay. Luciferase activity is shown as relative luciferase activity (RLA) compared with that in cells with the control vector. Transfection efficiency was normalized by co-transfection with pRL-TK. FOP-Flash was used as the negative control. Data show mean ± SD. Circles represent biological replicates ($n = 3$). For (H), data show mean ± SD. Circles represent biological replicates ($n = 6$). For (J), representative ChIP-qPCR experiments. Circles represent biological replicates ($n = 3$). For all panels, the ectopic or basal expression of NEURL in cell lines we tested in Fig 4 is shown in Fig EV1D–G; statistical significance was assessed by two-sided Student's *t*-tests, $^{*}P < 0.05$, $^{**}P < 0.01$ and $^{***}P < 0.001$; data show mean ± SD.
Source data are available online for this figure.

MG132. In NEURL-expressing HCT116 cells, β-catenin expression was barely detectable, presumably due to NEURL-mediated degradation. However, this degradation was blocked by MG132 (Fig EV4C). These results suggest that the degradation of β-catenin by NEURL is mediated through the ubiquitination–proteasome pathway.

Phosphorylation of β-catenin by GSK3β followed by binding with β-TrCP results in β-catenin degradation in the canonical Wnt pathway. We tested whether the involvement of NEURL in β-catenin degradation requires GSK-3β or β-TrCP. A pharmacological GSK3β inhibitor, 6-bromoindirubin-3′-oxime (BIO), that specifically inhibits GSK3β activity and inactivates the destruction complex was used, and the results showed an accumulation of active β-catenin (Meijer *et al*, 2003). Stable overexpression of NEURL in HCT116 cells reduced β-catenin protein levels and decreased its activity in response to BIO treatment by immunofluorescence and immunoblot analyses (Fig 5A and C). In contrast to the HCT116 cells, RKO cells showed extremely low basal β-catenin levels, due to the functional Axin destruction complex (Costa *et al*, 1999; Ou *et al*, 2011). However, BIO induced stable β-catenin expression in the cytoplasm and nucleus of RKO cells. The RKO cells were found to have an accumulation of active β-catenin in the presence of BIO. Consequently, transient transfection assays with WT NEURL and mutant NEURL lacking the RING domain were conducted. Overexpression of NEURL decreased the level of β-catenin, but transfection with inactive NEURL lacking the RING domain did not (Figs 5B and EV4D). These data suggest that NEURL-mediated negative regulation of β-catenin protein is independent of GSK3β activity.

Since our results showed that NEURL prompted the degradation of β-catenin independently of GSK3β activity, the degradation of β-catenin mediated by NEURL may occur via a mechanism distinct from β-TrCP1. To test this hypothesis, we blocked β-TrCP1 activity using small interfering RNA (siRNA)-targeted depletion of β-TrCP1 in stably overexpressing NEURL HCT116 cells. Interestingly, β-TrCP1 had no additional effect on the NEURL-mediated β-catenin degradation (Fig 5D and E) and its target genes (Fig EV4E and F). As a follow-up to this, we observed that NEURL itself significantly suppressed β-catenin transcriptional activity in the HCT116 cells stably overexpressing NEURL plus depleted with β-TrCP1 (Fig 5F). Consistent with these observations, we verified that neither β-TrCP1 nor β-TrCP2 had an impact on NEURL-mediated β-catenin degradation in BIO-treated RKO cells (Fig 5G). Additionally, the depletion of both β-TrCP1 and β-TrCP2 by siRNAs did not affect NEURL-mediated β-catenin degradation in BIO-free RKO cells (Fig EV4G). Collectively, these findings suggest that NEURL-mediated β-catenin degradation does not require functional GSK3β or β-TrCP.

Clinical implications of NEURL and β-catenin levels for CRC

To determine if our findings have clinical relevance, we examined NEURL and β-catenin expression levels in serial sections of 98 primary CRCs specimens using immunohistochemistry (IHC) analysis. Loss of NEURL expression was observed in 18% (17 of 93) of the surgically resected colorectal adenocarcinomas. Intact NEURL expression was observed in the stained cytoplasmic β-catenin, while no NEURL expression was associated with stained nuclear β-catenin. The representative IHC data suggest that the level of NEURL was inversely correlated with the level of active β-catenin expression in the CRC tumours (Fig 6A). The gene expression profiles for the CRC patients from the TCGA database showed that the level of NEURL was inversely correlated with β-catenin expression in human CRC samples ($n = 216$) and the results were statistically significant ($R = -0.243$; $P = 0.000323$) (Fig 6B). Moreover, Kaplan–Meier analysis showed that CRC patients with NEURL expression loss (5-year survival rate, 50.5%) are associated with shorter survival times than patients with NEURL expression (79.0%; $P = 0.069$, log = rank test; Fig 6C). Strikingly, recurrence-free survival in CRC patients with NEURL expression loss (5-year survival rate, 27.5%) was significantly worse than that of patients with intact NEURL expression (64.1%; $P = 0.027$, log = rank test; Fig 6D). These data strongly suggest that NEURL is inversely correlated with active β-catenin and could be a potential prognostic marker and new therapeutic target for CRC patients.

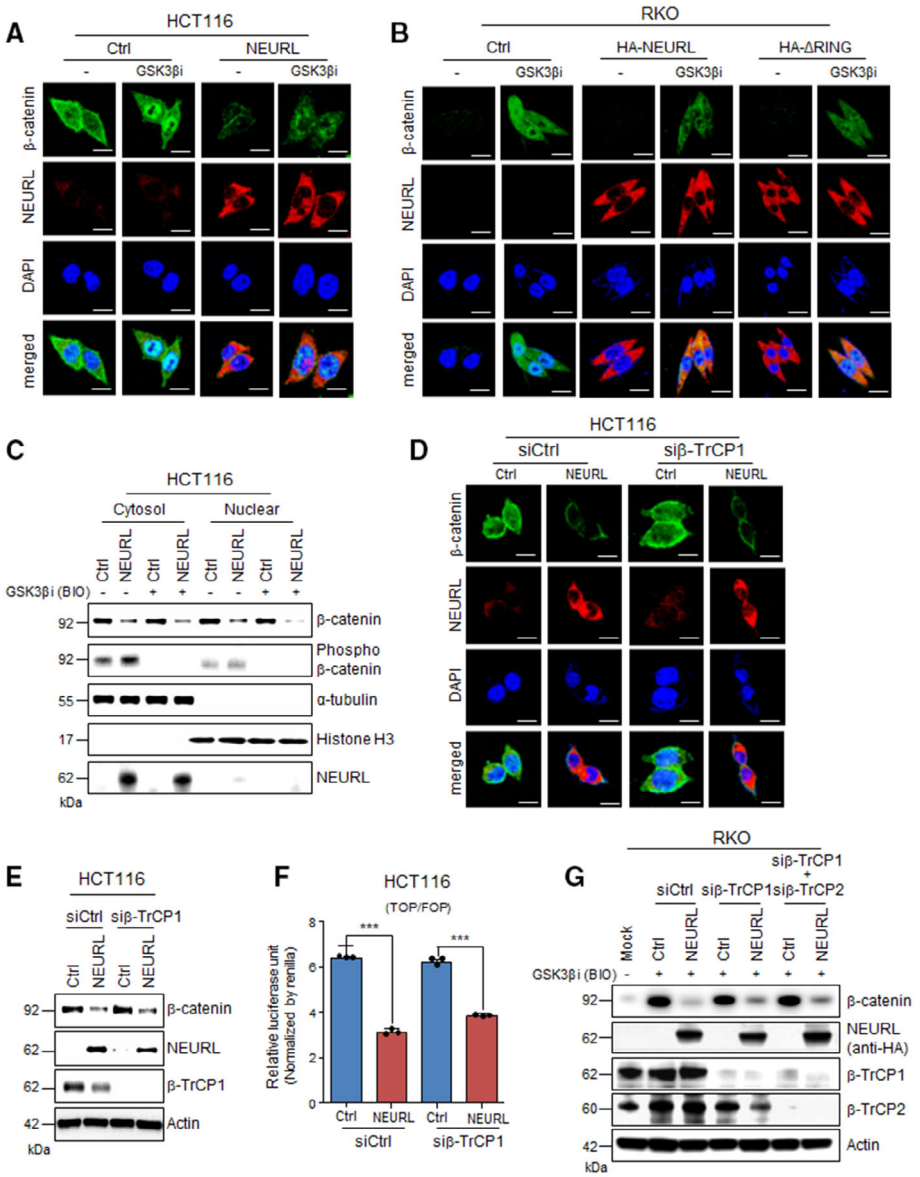

Figure 5. Destabilization of β-catenin by NEURL is GSK3β or β-TrCP independent.

A, B IF staining of β-catenin (green) or NEURL (red) in (A) HCT116 cells stably expressing NEURL or control cells with the indicated treatments and (B) RKO cells that were transiently transfected with the indicated plasmids and treatments. DAPI (blue) was used to stain the nuclei. Treatments were conducted with the glycogen synthase kinase-3β (GSK3β) inhibitor (BIO, 5 μM) for 3 or 24 h respectively. Confocal microscopy was performed. Scale bar, 10 μm.

C IB analysis of β-catenin levels in the cytosol and nucleus with or without BIO (5 μM, 24 h) in HCT116 cells stably overexpressing NEURL and the control cells. Cell fractions were prepared from HCT116 cells stably expressing NEURL or the empty vector. Cytosolic fractions and nuclear fractions were probed for β-catenin and NEURL expression. Alpha-tubulin and histone H3 served as loading controls and cell fraction markers.

D IF staining of β-catenin (green) or NEURL (red) in HCT116 cells that stably overexpressed NEURL and were transfected with β-transducin repeat-containing protein (β-TrCP) small interfering RNA (siRNA), or control siRNA. Scale bar, 10 μm.

E IB analysis shows that the β-catenin levels depend on NEURL expression transfected with β-TrCP siRNA or control siRNA in HCT116 cells.

F Relative TOP/FOP activities depend on NEURL expression transfected with β-TrCP siRNA or control siRNA in HCT116 cells. Luciferase activity was measured at 48 h after transfection using the dual-luciferase assay. Luciferase activity is shown as relative luciferase activity (RLA) when compared with the cells in control vector. FOP-Flash was used as the negative control. Statistical significance was assessed by two-sided Student's *t*-test, $^{***}P < 0.001$; $n = 3$, biological replicates; data show means ± SD.

G IB analysis of the β-catenin levels in RKO cells (after BIO treatment, 5 μM, 24 h) with or without NEURL expression (i.e. transfected with β-TrCP1, β-TrCP2 siRNA or control siRNA).

Source data are available online for this figure.

Discussion

This study has identified an epigenetic event that contributes to aberrant Wnt/β-catenin signalling in human colorectal cancer. Specifically, we have provided epigenetic, cellular function and mechanistic data to demonstrate that *NEURL* is a tumour suppressor in colorectal cancer. Overall, the results have established that NEURL is a potentially important target for cancer therapies designed to control aberrant Wnt/β-catenin signalling. Promoter CpG island hypermethylation in tumour suppressor genes is a common hallmark of human cancers (Baylin & Jones, 2016). Recent comprehensive DNA methylation microarrays and genome-wide bisulphite sequencing have identified not only an individual gene but also a signature that is associated with various cancers, indicating the potential use of biomarkers for cancer detection and prognosis (Heyn & Esteller, 2012). The methylation frequencies of *NEURL* in CRC are relatively lower than those of other known genes, such as SFRP genes, whose expression is frequently highly silenced by promoter hypermethylation (Suzuki *et al*, 2004; Liu *et al*, 2019). Despite the lower hypermethylation frequency of *NEURL* in primary CRC patients, we have provided evidence that patients with epigenetically silenced *NEURL* are associated with poor clinical outcomes based on the TCGA database analysis. Moreover, IHC data from TMA showed that a NEURL deficiency in CRC is associated with poor outcomes and a lower level of recurrence-free survival. This strongly supports the idea that epigenetically silenced NEURL may be a suitable biomarker for the prognosis of colon cancer.

Although there has been a growing list of hypermethylated genes that may be considered tumour suppressor candidates, the biological significance of these genes remains still unknown. The function of NEURL, however, in the Notch pathway has been well characterized in both *Drosophila* and *Xenopus* (Deblandre *et al*, 2001; Lai *et al*, 2001; Pavlopoulos *et al*, 2001; Yeh *et al*, 2001). For mammalian NEURL, several mouse models with specific defects in olfactory discrimination and hypersensitivity to ethanol (Ruan *et al*, 2001), as well as defects in spermatogenesis and mammary gland maturation (Vollrath *et al*, 2001), have been reported. In addition, no functional NEURL data have been reported to date. Therefore, this study is the first to describe NEURL as a tumour suppressor that targets β-catenin leading to aberrant Wnt/β-catenin signalling.

Here, we show that NEURL interacts with β-catenin to induce the aberrant Wnt/β-catenin signalling pathway, which then suppresses tumour cell proliferation and interrupts tumorigenesis. Recent studies have shown that several E3 ligases target β-catenin degradation via the Wnt-dependent pathway. Interestingly, these ligases predominantly degrade β-catenin in the cytosol during the Wnt-off phase (β-TrCp and Jade-1), in specific cell types (*Ozz* in developing myocytes), and in response to unique stimuli (Siah-1 in the DNA damage pathway) (Liu *et al*, 2001; Nastasi *et al*, 2004; Chitalia *et al*, 2008). Recently, a new RING domain associated with E3 ligases, including c-Cbl and TRIM33, that targets nuclear β-catenin degradation was identified (Chitalia *et al*, 2013; Xue *et al*, 2015). Our data demonstrate that NEURL degraded the majority of the cytoplasmic β-catenin in colon cancer cells in which the Wnt pathway was constitutively activated. This effect strongly supports the idea that NEURL is an E3 ligase and plays a critical role in facilitating tumour-suppressive activity via β-catenin downregulation. Moreover, NEURL-induced β-catenin degradation did not require functional β-TrCP, which is required for β-catenin degradation in the canonical Wnt pathway. Furthermore, similar to β-TrCp, Jade-1 and TRIM33, NEURL has been identified as a negative regulator of the Wnt pathway. These findings suggest that NEURL is a novel E3 ligase target for β-catenin and important for the pathophysiology of the canonical Wnt signalling pathway. Our discoveries reveal that the interactions between NEURL and β-catenin induce β-catenin degradation, interrupting the constitutive activation of Wnt signalling in colon cancer cells, resulting in a tumour-suppressive effect. Importantly, the downregulation or inactivation of NEURL by promoter hypermethylation in CRC results in the constitutive activation of the Wnt signalling pathway, which facilitates tumorigenesis (Fig 6E).

Here, we hypothesize that NEURL may have a biological role independent of the Notch signalling pathway in mammalian cells. Koo *et al* (2007) have addressed the fact that there have been no obvious Notch signalling defects identified when using NEURL1 and NEURL2 knockout mice. In agreement with this report, we have not observed any Notch signalling associated with NEURL overexpression in cancer cells when assessing Notch luciferase activity, which supports the hypothesis that NEURL has a novel function outside the Notch pathway. Herein, this function was further identified as a novel tumour suppressor in human cancer.

NEURL is predominantly located in the cytoplasm of cancer cells, suggesting that it may interact in the cytoplasm with other molecules, affecting their function. Recently, multiple reports have suggested a novel non-canonical role for Notch as an antagonizer of the Wnt/β-catenin signalling, which is a critical regulator of development and disease, irrespective of the Notch ligand-dependent cleavage or nuclear localization (Hayward *et al*, 2005; Kwon *et al*, 2011). NEURL-mediated β-catenin degradation that contributes to tumorigenesis can also be explained by a non-canonical Notch signalling (Andersen *et al*, 2012). However, further experiments are required to determine the exact mechanisms by which components of the notch signalling promote β-catenin degradation.

Recently, DVL has been reported as a cytoplasmic scaffold that promotes processes such as β-catenin stabilization (Gao & Chen, 2010) and it has also been shown that nuclear localization of DVL is important for canonical signalling (Itoh *et al*, 2005; Gan *et al*, 2008). Interestingly, recently it was uncovered that the DVL proteins such as DVL1 and DVL3 might play a role in mediating aberrant Wnt signalling and promoting tumorigenesis (Castro-Piedras *et al*, 2018, 2021; Sharma *et al*, 2019). Since we were the first to report a novel biological function of NEURL as tumour suppressor in a cancer model, we hypothesize that NEURL could serve as a biological link along with DVL in regulating Wnt pathway as well as tumour progression.

Beta-catenin can be activated by multiple pathways, including Wnt-dependent and Wnt-independent pathways, and is an emerging key molecule in the pathogenesis of various cancers (Yu *et al*, 2021; Chatterjee *et al*, 2022). Along with recent findings which show that E3 ligases can strongly target β-catenin, our functional data also support the idea that NEURL plays an important role in Wnt/β-catenin pathway dysregulation. Moreover, identifying E3 ubiquitin ligases that can target β-catenin through multiple pathways is critical for developing pharmacological targets that can modulate β-catenin activity in cancer. Our clinical data strongly support the idea

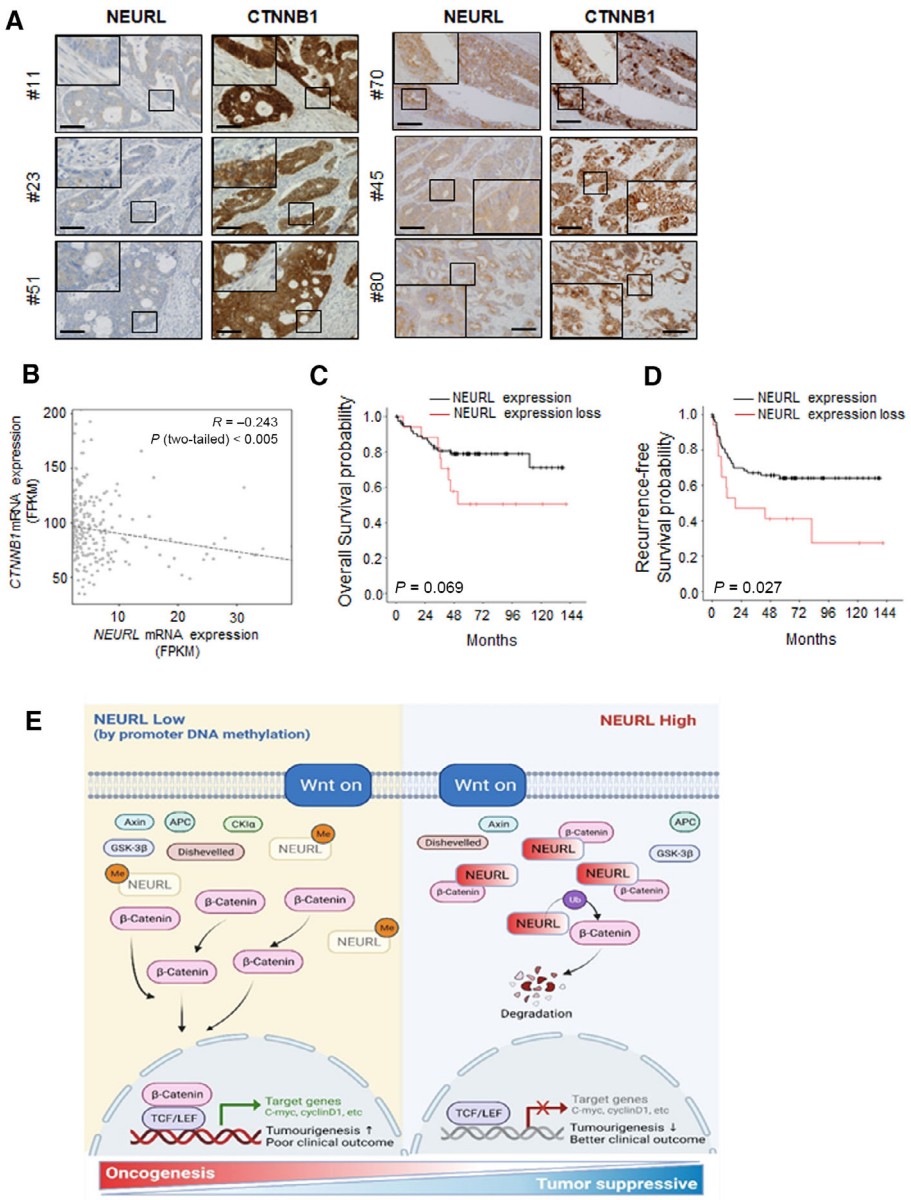

Figure 6. Clinical outcomes of NEURL expression correlated with β-catenin in CRC patients.

A IHC analysis of NEURL expression and β-catenin levels in primary CRC specimens. Representative images of NEURL and β-catenin expression in adenocarcinomas from the colorectum. Left panels; loss of NEURL expression and nuclear β-catenin labelling (Patient no: #11/23/51). Intact NEURL expression and cytoplasmic β-catenin labelling (Patient no: #70/45/80). Right panels: patients with intact NEURL expression tended to show cytoplasmic β-catenin labelling, while those with a loss of NEURL expression were associated with nuclear β-catenin labelling. The boxed regions are displayed at high magnification in the inset (Scale bar, 100 μm).

B Correlation analysis of the association between NEURL and CTNNB1 gene expression in the TCGA-COAD dataset ($R = -0.243$; $P = 0.000323$). Statistical significance was determined by Spearman's correlation test.

C, D Kaplan–Meier survival analyses for colorectal carcinoma patients ($n = 93$) in relation to NEURL expression. (C) Overall survival time in colorectal cancer patients with NEURL expression loss (5-year survival rate, 50.5%) tended to be shorter compared to those with intact NEURL expression (79.0%; $P = 0.069$). (D) Recurrence-free survival time in colorectal cancer patients with NEURL expression loss (5-year survival rate, 27.5%) was significantly worse compared to those with intact NEURL expression (64.1%; $P = 0.027$). Statistical significance was performed by log-rank test.

E Working model describing how NEURL can regulate β-catenin stability in Wnt signalling. Left panel: Wnt treatment induces canonical Wnt/β-catenin signalling pathway activation and stabilized β-catenin. Stabilized β-catenin that is translocated to the nucleus forms a complex with TCF/LEF-1 transcription factors, which controls the expression of many target genes, such as *c-myc* and *Cyclin D1*. In this case, NEURL is silenced by promoter DNA hypermethylation, resulting in constitutive activation of the Wnt signalling pathway to promote tumour cell proliferation and facilitate tumorigenesis. Right panel: When NEURL is expressed, our data have demonstrated that the constitutively active Wnt/β-catenin pathway can be suppressed by β-catenin degradation through ubiquitination because of the interaction between NEURL and β-catenin in the cytosol, which results in the suppression of tumorigenesis.

Source data are available online for this figure.

that NEURL and β-catenin may represent therapeutic targets for colorectal cancer.

However, this study has certain limitations, and some aspects require further investigation. DLD1, SW480 and HCT116 cells are Wnt-dependent cancer cell lines (Chen *et al*, 2009), while RKO cell is a Wnt-independent cancer cell, which has an intact β-catenin degradation system, making β-catenin undetectable by Immunoblot (Costa *et al*, 1999; Ibrahem *et al*, 2014). To make β-catenin detectable, we treated the RKO cells with GSK3β inhibitor (BIO) to determine whether NEURL could decrease the level of β-catenin. Our data suggest that GSK3β inhibitor successfully rendered β-catenin detectable and NEURL decrease of the level of β-catenin. Although we confirmed that NEURL overexpression could degrade β-catenin stabilized upon treatment with GSK3β inhibitor, current data do not fully support the evidence of how tumour growth suppression by NEURL overexpression in RKO cells is associated with Wnt signalling pathway. Therefore, the tumour-suppressive function of NEURL in RKO cells may be independent of the Wnt/β-catenin pathway; however, further studies are necessary to clarify the precise mechanism. Additionally, the effects of loss of NEURL function in NEURL KO model remain to be elucidated. Notably, Clevers and other research groups have already identified both ZNFR3 and RNF43 as Wnt signalling inhibitors through the use of genetic deletion models, proposing their involvement as tumour suppressors (Hao *et al*, 2012; Koo *et al*, 2012). However, it is crucial to investigate the molecular mechanisms underlying NEURL's function in colon cancer. Moreover, future investigations should aim to unravel the role of NEURL in cancer progression.

In summary, this study identified that epigenetically regulated NEURL is a critical regulator of the Wnt/β-catenin pathway. The restoration of NEURL repressed cellular proliferation and tumorigenesis by interrupting the canonical Wnt/β-catenin pathway in colon cancer. Since the biological importance of NEURL as a novel tumour suppressor is functionally relevant to the Wnt/β-catenin pathway in human cancers; these findings provide not only an advanced understanding of the molecular mechanisms that underlie the aberrant Wnt/β-catenin pathway, but also suggest potential clinical targets for therapeutic interventions.

Materials and Methods

Plasmids, small interfering RNAs (siRNAs) and reagents

Complementary DNA (cDNA) encoding full-length human *Neuralized* (*NEURL*) was amplified by reverse transcription-polymerase chain reaction (RT-PCR) from normal colon RNA (Stratagene). For mammalian expression constructs, wild-type (WT) NEURL and its inactive mutant were cloned into the pIRES-Neo3 vector (Invitrogen). HA containing WT NEURL and its inactive mutant were also cloned into the pEF1α-IRES-puro vector. NEURL siRNA, β-transducin repeat-containing protein (β-TrCP1) siRNA and a non-target siRNA (siControl) were purchased from Dharmacon. β-TrCP2 siRNA was purchased from Santa Cruz Biotechnology. Recombinant human Wnt3a was purchased from R&D System. Cycloheximide (CHX), MG132, LiCl, cisplatin, leptomycin B and mitomycin C were purchased from Sigma-Aldrich. The glycogen synthase kinase-3 beta (GSK3β)-specific inhibitor was purchased from Selleckchem.

Generation of a stable cell line

The NEURL cDNA was subcloned into the mammalian expression vector pIRES-NEO3 (Invitrogen) and pEF1α-puro containing a HA tag and a neomycin or puromycin resistance gene to establish stable transfectants. Individual clones were selected and maintained in the presence of G418 (4 μg/ml) or puromycin (2 μg/ml). Selected clones expressing NEURL or HA were detected by western blot analysis. Stable control colonies were also generated in parallel.

Cell culture and transfection with plasmids

Human colorectal carcinoma cell lines (HCT116, SW480, RKO, Colo320 and DLD1) and a human embryonic kidney cell line (293T) were obtained from the American Type Culture Collection (ATCC). The related experiments were completed within 6 months of purchasing the cell lines and subjected to routine microscopic inspection to ensure a stable phenotype. HCT116 and SW480 cells were maintained in McCoy's 5A medium (WelGENE). RKO and 293T cells were cultured in Dulbecco's Modified Eagle's Medium (DMEM; WelGENE). Colo320 and DLD1 cells were maintained in RPMI medium (WelGENE). All culture media were supplemented with 10% foetal bovine serum (FBS; Hyclone) and 1% antibiotic–antimycotic (Gibco). HCT116, SW480, RKO and 293T cells were transfected with Lipofectamine 2000 (Invitrogen). HCT116 and SW480 cells were transfected with siRNAs using Lipofectamine RNAi MAX (Invitrogen).

Cell proliferation and colony formation assay

Cell proliferation was determined by 3-(4,5-dimethylthiazol-2-yl)-2,5-diphenyltetrazolium bromide assays (Promega) as previously described (Kim *et al*, 2014). For the colony formation assay, cells were plated at a density of 5×10^3 cells per well in a six-well plate. The staining, visualization and counting of triplicate wells were performed as previously described (Kim *et al*, 2014).

Migration and invasion assay

Cell migration was determined using 24-well transwell plates (8-μm pore size, Corning Costar), and the invasion assay was carried out using a Matrigel-coated invasion chamber (24 wells, 8-μm pore size, Corning Costar). The upper chamber contained cells in specific media with 1% FBS, and the lower chamber contained media with 10% FBS. Cells were incubated for 16 h at 37°C in 20% O_2 and 5% CO_2. Non-migrated or non-invasive cells were scraped off the upper membrane with a cotton swab. Migrated or invasive cells that remained on the bottom membrane were counted after staining with Giemsa (Sigma-Aldrich). Photographs were taken using a Qicam image camera system that was mounted on a Nikon ECLIPSE 80i microscope (Nikon).

Western blot analysis

Lysates containing equal amounts of protein were resolved using 4–12% Bis-Tris gel (Invitrogen, MA, USA) electrophoresis and then transferred to polyvinylidene difluoride membranes (GE Healthcare Life Sciences). The membranes were incubated overnight at 4°C

with specific primary antibodies against NEURL (SAB2108366, Sigma), Histone H3 (ab1791, Abcam), survivin (ab469, Abcam), Delta-like 1 (ABIN375140, Antibodies-online GmbH), β-catenin (610154, BD Biosciences), β-transducin repeat-containing protein (β-TrCP1) (#4394S, Cell Signaling), phospho-β-catenin (Ser33/37/Thr41; #9561S, Cell Signalling), cyclin D1 (sc-246, Cell Signaling), HA (sc-7392, Santa Cruz Biotechnology), Flag (F3165, Sigma), 6X His tag (ab18184, Abcam), α-tubulin (F3165, sc-8035, Santa Cruz Biotechnology), Axin2 (20540-1-AP, Proteintech), Actin (612656, BD Biosciences), GAPDH (sc-365062, Santa Cruz Biotechnology), c-Myc (sc-40, Santa Cruz Biotechnology), Claudin1 (sc-17658, Santa Cruz Biotechnology), Frizzled7 (sc-31061, Santa Cruz Biotechnology), GSK-3α/β (sc-7291, Santa Cruz Biotechnology), Jagged-1 (sc-390177, Santa Cruz Biotechnology), Snail (ab31787, Abcam), SOX9 (sc-166505, Santa Cruz Biotechnology) and β-TrCP2 (sc-166492, Santa Cruz Biotechnology).

Tissue samples

A total of 43 primary colorectal cancer specimens were obtained, as was previously described (Yamamoto *et al*, 2012). Samples of adjacent normal colorectal mucosa were also collected from 34 patients. All H&E-stained slides from 93 surgically resected colorectal cancers were carefully reviewed (Asan Medical Center, Korea). Areas of normal colonic epithelia and adenocarcinomas were identified. Data including sex, age, other accompanying tumours, and the results of the most recent follow-up examination were collected by reviewing patient medical records. Pathological characteristics that were evaluated included tumour location and size, histological subtype, differentiation, depth of invasion, lymphovascular and perineural invasion, lymph node and distant metastases. All elements of this study were approved by the institutional review boards of Sapporo Medical University (IRB no. 24-04, Sapporo, Japan) and Asan Medical Center, University of Ulsan College of Medicine (IRB no. 2022-0771, Seoul, Korea), and written informed consent was obtained from all patients.

The Cancer Genome Atlas (TCGA) data analysis

Genome-wide DNA methylation and expression data for colon cancer samples profiled by TCGA-COAD (Colon Adenocarcinoma) datasets obtained from GDC (Genomic Data Commons) data portal (NCI, https://portal.gdc.cancer.gov/). Level 3 datasets that were obtained through the Infinium HumanMethylation450 BeadChip were analysed using the R software (http://www.R-project.org/). Survival analysis was carried out using the Cutoff Finder website (http://molpath.charite.de/cutoff/).

Co-immunoprecipitation (Co-IP)

Co-immunoprecipitation was performed as previously described (Park *et al*, 2015). Briefly, for immunoprecipitation experiments, 500-μg lysates were incubated with 1 μg of the appropriate antibody that was conjugated to Protein A/G-agarose beads (Sigma) for 12 h at 4°C with rotation. After washing with lysis buffer, the proteins were eluted from the beads by boiling in sodium dodecyl sulphate (SDS) sample buffer and resolved on 10% SDS-polyacrylamide gel electrophoresis, after which they were subjected to immunoblotting with the appropriate antibodies.

Dual-luciferase assay

HCT116 and 293T cells were transfected with FOP- and TOP-FLASH reporter plasmids, along with pRK-TK. Luciferase activity was measured using a Dual-Luciferase reporter Assay Kit (Promega), according to the manufacturer's protocol. Relative renilla luciferase activity was used for transfection efficiency and normalization of firefly luciferase activity.

Chromatin immunoprecipitation (ChIP)

Chromatin immunoprecipitation assays were performed as previously described (Barlev *et al*, 2001). PCR was performed using a CFX96™ Real-Time System (BioRad). The ChIP primers are listed in Table EV1. A β-catenin antibody (BD Biosciences) was used to immunoprecipitate β-catenin-associated chromatin fragments.

Xenograft analysis

Female BALB/c nude mice (4 weeks old) were obtained from Central Lab. Animal Inc (Seoul, Korea). For the HCT116 cells, 15 nude mice were randomly divided into three groups (mock; $n = 5$, empty vector control; $n = 4$, and NEURL overexpression; $n = 5$), and 5×10^6 cells were inoculated subcutaneously into each mouse. For SW480 cells, 42 nude mice were randomly assigned into six groups (untreated, treated with cisplatin [3 mg/kg by intraperitoneal (i.p.) injection after 1 week], or treated with mitomycin C [3 mg/kg by i.p. injection after 1 week]; $n = 7$ for each group). Tumours were monitored every week, and the tumour volume was estimated as follows: tumour volume = $(\text{short axis})^2 \times (\text{long axis}) \times 0.5$. Following the experiment, we sacrificed the mice and excised and weighed the tumours. All animal housing and experimental procedures were approved by the Institutional Animal Care and Use Committee of the Center for Laboratory Animal Sciences (HYI-17-261-1), Medical Research Coordinating Center, and the HYU Industry-University Cooperation Foundation.

Immunofluorescence

HCT116 control and NEURL-overexpressing cells, as well as the SW480 (control) and NEURL KD cells, were fixed with 4% paraformaldehyde for 10 min. Cells were then washed three times with PBS containing 0.1% Triton X-100 (PBST), permeabilized in 0.5% Triton X-100 in PBS, and washed once in PBST. Subsequently, cells were blocked in 20% FBS in PBS for 30 min and then, incubated with the anti-NEURL and anti-β-catenin antibodies for 1 h at 37°C. The cells were then washed with PBS and incubated with an anti-rabbit IgG-Alexa Flour 594 antibody (A-11012, Invitrogen) or an anti-mouse IgG-FITC or Cy3 antibody (31569, M30010, Invitrogen) for 1 h. After rinsing in PBS, Hoechst 33342 or 4′,6-diamidino-2-phenylindole (DAPI; D9542, Sigma Aldrich) was added to slides to counterstain the nuclei. Slides were washed with PBS and mounted using Vectashield (Vector Laboratories). Images were captured with either an LSM700 confocal microscope (Zeiss) or a Nikon Eclipse Ni-U microscope using a DS-Fi2 digital camera (Nikon), which was supported by the NIS-Elements BR 4.00.03 software (Nikon).

Construction of tissue microarrays

Tissue microarrays were constructed from formalin-fixed paraffin-embedded tissue blocks of 94 surgically resected colorectal cancers with a manual tissue microarrayer (UniTMA Co Ltd). Areas containing > 75% cancer cells without accompanying necrosis were selected. The tissue array blocks contained four cores from cancers, as well as either four cores from primary colorectal cancers or two from primary and two from colorectal cancers metastasis to other organs, and one core from normal colonic mucosa.

Immunohistochemistry (IHC)

Serial 4-μm sections were applied to 3-aminopropyltriethoxy-sialne-coated slides (Sigma), deparaffinized and rehydrated in xylene and serially diluted ethanol. Endogenous peroxidase was blocked by incubation in a 3% solution of aqueous hydrogen peroxide, after which heat-induced antigen retrieval was performed. Primary antibodies for β-catenin (1:2,000; 13-8400, Invitrogen) and NEURL (1:800; CPA2360; Cohesion Biosciences) with Benchmark autostainer (Ventana Medical Systems) were used following the manufacturer's protocol. The primary antibody was incubated at RT for 32 min, after which the sections were labelled using an automated immunostaining system with an I-View detection kit (Ventana Medical Systems). Immunostained sections were lightly counterstained with haematoxylin, dehydrated in ethanol, and cleared in xylene.

Construction of β-catenin DNA plasmids

The human β-catenin-EGFP was purchased from Addgene. The pmScarlet-I_C1 vector was provided by Drs. Seong JH (Korea Institute of Science and Technology, Seoul, Republic of Korea). The mScarlet-I was amplified by PCR using Phusion High-Fidelity DNA polymerase (Thermo Scientific) and inserted into human β-catenin-EGFP by NheI (Thermo Scientific) and KpnI (Thermo Scientific) sites. The primers are forward 5′-aaa tgc tag cgc cac cat ggt gag caa ggg c-3′ and reverse 5′-gta cgg tac cct tgt aca gct cgt cca tgc-3′. The mScarlet-I-β-catenin-EGFP S33Y mutant was generated by using Site-directed Mutagenesis Kit (Enzynomics). The primers are forward 5′-agc aac agt ctt acc tgg act atg gaa tcc att ctg-3′ and reverse 5′-cag aat gga ttc cat agt cca ggt aag act gtt gct-3′.

Transfection and fixation

The DNA plasmids were transfected into the cells by using Lipofectamine 3000 (Invitrogen) reagent according to the product instructions. The cells were fixed with 4% paraformaldehyde in PBS (Biosesang) for 10 min at room temperature, followed by washing three times with PBS. The fixed cells were stained with Hoechst 33342 (Invitrogen). After washing five times with PBS, the samples were mounted in the made-mounting solution (0.1 M TRIS buffer (pH 9.0) 5 ml, n-propyl gallate (0.25 g), glycerol 45 ml).

Image acquisition and confocal microscopy

Confocal images were acquired using a Zeiss laser scanning confocal microscopy (LSM-800) with a 40× C-Apochromat objective/numerical aperture (NA) 1.2 water immersion and a 63× plan-apochromat objective/numerical aperture (NA) 1.40 oil immersion. The diode laser lines were with 405, 488 and 561 nm laser wavelength. The excitation filter sets were, respectively, 365, 450–490 and 546/12 nm. The beamsplitter (BS) filter sets were 395, 510 and 560 nm respectively. The emission filter sets were used with 445/50, 515–565 and 575–640 nm respectively.

Statistical analysis

Statistical analyses were performed using SPSS version 17.0 available for Windows OS (Chicago, IL, USA). To compare any associations between the immunohistochemical markers and clinicopathological parameters, the χ^2 and Fisher's exact tests were used. The significance of the data between two experimental groups was determined by Student's *t*-test, and multiple group comparisons were analysed by one-way ANOVA. All statistical analyses were two-sided, and data were considered statistically significant based on the *P*-values such as $P < 0.05$ (*), $P < 0.01$ (**) and $P < 0.001$ (***).

Data availability

No primary datasets have been deposited.

Expanded View for this article is available online.

Acknowledgements

Funding was supported by the National Research Foundation of Korea (NRF) grant funded by the Korean Government (MSIT) (NRF-2019R1A2C1008502, NRF-2020M2C8A2069356, NRF-2021M2E8A1049300 and NRF-2021R1G1A1093784).

Author contributions

Joo Mi Yi: Conceptualization; supervision; funding acquisition; validation; investigation; writing – original draft; project administration; writing – review and editing. **Tae-Hong Kang:** Data curation; formal analysis; investigation; visualization; methodology; writing – original draft. **Yu Kyeong Han:** Data curation; formal analysis; visualization; methodology. **Ha Young Park:** Data curation; formal analysis; visualization; methodology. **Ju Hwan Yang:** Data curation; formal analysis; visualization; methodology. **Jin-Han Bae:** Data curation; formal analysis; visualization; methodology. **Jung-Soo Suh:** Data curation; formal analysis; visualization; methodology. **Tae-Jin Kim:** Data curation; formal analysis; visualization. **Joong-Gook Kim:** Data curation; formal analysis; visualization; methodology. **Yan-Hong Cui:** Data curation; formal analysis; visualization; methodology. **Hiromu Suzuki:** Data curation; formal analysis; visualization; methodology. **Kohei Kumegawa:** Data curation; formal analysis; methodology. **Sung Joo Kim:** Data curation; formal analysis; methodology. **Yi Zhao:** Formal analysis; methodology. **In Ja Park:** Formal analysis; methodology. **Seung-Mo Hong:** Data curation; formal analysis; validation; methodology. **Joon-Yong Chung:** Data curation; formal analysis; visualization; methodology. **Su-Jae Lee:** Conceptualization; supervision; investigation; writing – original draft; writing – review and editing.

Disclosure and competing interests statement

The authors declare that they have no conflict of interest.

References

Aguilera O, Fraga MF, Ballestar E, Paz MF, Herranz M, Espada J, Garcia JM, Munoz A, Esteller M, Gonzalez-Sancho JM (2006) Epigenetic inactivation of the Wnt antagonist DICKKOPF-1 (DKK-1) gene in human colorectal cancer. *Oncogene* 25: 4116 – 4121

Andersen P, Uosaki H, Shenje LT, Kwon C (2012) Non-canonical Notch signaling: emerging role and mechanism. *Trends Cell Biol* 22: 257 – 265

Barlev NA, Liu L, Chehab NH, Mansfield K, Harris KG, Halazonetis TD, Berger SL (2001) Acetylation of p53 activates transcription through recruitment of coactivators/histone acetyltransferases. *Mol Cell* 8: 1243 – 1254

Baylin SB, Jones PA (2016) Epigenetic determinants of cancer. *Cold Spring Harb Perspect Biol* 8: a019505

Boulianne GL, de la Concha A, Campos-Ortega JA, Jan LY, Jan YN (1991) The *Drosophila* neurogenic gene neuralized encodes a novel protein and is expressed in precursors of larval and adult neurons. *EMBO J* 10: 2975 – 2983

Brock MV, Hooker CM, Ota-Machida E, Han Y, Guo M, Ames S, Glockner S, Piantadosi S, Gabrielson E, Pridham G *et al* (2008) DNA methylation markers and early recurrence in stage I lung cancer. *N Engl J Med* 358: 1118 – 1128

Bugter JM, Fenderico N, Maurice MM (2021) Mutations and mechanisms of WNT pathway tumour suppressors in cancer. *Nat Rev Cancer* 21: 5 – 21

Cancer Genome Atlas Network (2012) Comprehensive molecular characterization of human colon and rectal cancer. *Nature* 487: 330 – 337

Castro-Piedras I, Sharma M, den Bakker M, Molehin D, Martinez EG, Vartak D, Pruitt WM, Deitrick J, Almodovar S, Pruitt K (2018) DVL1 and DVL3 differentially localize to CYP19A1 promoters and regulate aromatase mRNA in breast cancer cells. *Oncotarget* 9: 35639 – 35654

Castro-Piedras I, Sharma M, Brelsfoard J, Vartak D, Martinez EG, Rivera C, Molehin D, Bright RK, Fokar M, Guindon J *et al* (2021) Nuclear Dishevelled targets gene regulatory regions and promotes tumor growth. *EMBO Rep* 22: e50600

Chatterjee A, Paul S, Bisht B, Bhattacharya S, Sivasubramaniam S, Paul MK (2022) Advances in targeting the WNT/β-catenin signaling pathway in cancer. *Drug Discov Today* 27: 82 – 101

Chen B, Dodge ME, Tang W, Lu J, Ma Z, Fan C-W, Wei S, Hao W, Kilgore J, Williams NS *et al* (2009) Small molecule–mediated disruption of Wnt-dependent signaling in tissue regeneration and cancer. *Nat Chem Biol* 5: 100 – 107

Chitalia VC, Foy RL, Bachschmid MM, Zeng L, Panchenko MV, Zhou MI, Bharti A, Seldin DC, Lecker SH, Dominguez I *et al* (2008) Jade-1 inhibits Wnt signalling by ubiquitylating [beta]-catenin and mediates Wnt pathway inhibition by pVHL. *Nat Cell Biol* 10: 1208 – 1216

Chitalia V, Shivanna S, Martorell J, Meyer R, Edelman E, Rahimi N (2013) c-Cbl, a ubiquitin E3 ligase that targets active β-catenin: a novel layer of Wnt signaling regulation. *J Biol Chem* 288: 23505 – 23517

Clevers H (2004) Wnt breakers in colon cancer. *Cancer Cell* 5: 5 – 6

Clevers H, Nusse R (2012) Wnt/β-catenin signaling and disease. *Cell* 149: 1192 – 1205

Commisso C, Boulianne GL (2007) The NHR1 domain of neuralized binds delta and mediates delta trafficking and Notch signaling. *Mol Biol Cell* 18: 1 – 13

Costa LT, He T-C, Yu J, Sparks AB, Morin PJ, Polyak K, Laken S, Vogelstein B, Kinzler KW (1999) CDX2 is mutated in a colorectal cancer with normal APC/beta-catenin signaling. *Oncogene* 18: 5010 – 5014

Deblandre GA, Lai EC, Kintner C (2001) Xenopus neuralized is a ubiquitin ligase that interacts with XDelta1 and regulates Notch signaling. *Dev Cell* 1: 795 – 806

Gan X-Q, Wang J-Y, Xi Y, Wu Z-L, Li Y-P, Li L (2008) Nuclear Dvl, c-Jun, β-catenin, and TCF form a complex leading to stabiLization of β-catenin–TCF interaction. *J Cell Biol* 180: 1087 – 1100

Gao C, Chen Y-G (2010) Dishevelled: the hub of Wnt signaling. *Cell Signal* 22: 717 – 727

Hao H-X, Xie Y, Zhang Y, Charlat O, Oster E, Avello M, Lei H, Mickanin C, Liu D, Ruffner H *et al* (2012) ZNRF3 promotes Wnt receptor turnover in an R-spondin-sensitive manner. *Nature* 485: 195 – 200

Hayward P, Brennan K, Sanders P, Balayo T, DasGupta R, Perrimon N, Arias AM (2005) Notch modulates Wnt signalling by associating with Armadillo/β-catenin and regulating its transcriptional activity. *Development* 132: 1819 – 1830

He T-C, Sparks AB, Rago C, Hermeking H, Zawel L, da Costa LT, Morin PJ, Vogelstein B, Kinzler KW (1998) Identification of c-MYC as a target of the APC pathway. *Science* 281: 1509 – 1512

Heyn H, Esteller M (2012) DNA methylation profiling in the clinic: applications and challenges. *Nat Rev Genet* 13: 679 – 692

Huang S-MA, Mishina YM, Liu S, Cheung A, Stegmeier F, Michaud GA, Charlat O, Wiellette E, Zhang Y, Wiessner S *et al* (2009) Tankyrase inhibition stabilizes axin and antagonizes Wnt signalling. *Nature* 461: 614 – 620

Ibrahem S, Al-Ghamdi S, Baloch K, Muhammad B, Fadhil W, Jackson D, Nateri AS, Ilyas M (2014) STAT3 paradoxically stimulates β-catenin expression but inhibits β-catenin function. *Int J Exp Pathol* 95: 392 – 400

Itoh K, Brott BK, Bae G-U, Ratcliffe MJ, Sokol SY (2005) Nuclear localization is required for Dishevelled function in Wnt/β-catenin signaling. *J Biol* 4: 3

Katoh M (2017) Canonical and non-canonical WNT signaling in cancer stem cells and their niches: cellular heterogeneity, omics reprogramming, targeted therapy and tumor plasticity (review). *Int J Oncol* 51: 1357 – 1369

Katoh M, Katoh M (2022) WNT signaling and cancer stemness. *Essays Biochem* 66: 319 – 331

Kim J-G, Kim T-O, Bae J-H, Shim J-W, Kang MJ, Yang K, Ting AH, Yi JM (2014) Epigenetically regulated MIR941 and MIR1247 target gastric cancer cell growth and migration. *Epigenetics* 9: 1018 – 1030

Koo B-K, Yoon M-J, Yoon K-J, Im S-K, Kim Y-Y, Kim C-H, Suh P-G, Jan YN, Kong Y-Y (2007) An obligatory role of mind bomb-1 in Notch signaling of mammalian development. *PLoS One* 2: e1221

Koo B-K, Spit M, Jordens I, Low TY, Stange DE, van de Wetering M, van Es JH, Mohammed S, Heck AJR, Maurice MM *et al* (2012) Tumour suppressor RNF43 is a stem-cell E3 ligase that induces endocytosis of Wnt receptors. *Nature* 488: 665 – 669

Korinek V (1997) Constitutive transcriptional activation by a [beta]-catenin-Tcf complex in APC−/− colon carcinoma. *Science* 275: 1784 – 1787

Kwon C, Cheng P, King IN, Andersen P, Shenje L, Nigam V, Srivastava D (2011) Notch post-translationally regulates [beta]-catenin protein in stem and progenitor cells. *Nat Cell Biol* 13: 1244 – 1251

Lai EC, Rubin GM (2001) Neuralized functions cell-autonomously to regulate a subset of Notch-dependent processes during adult *Drosophila* development. *Dev Biol* 231: 217 – 233

Lai EC, Deblandre GA, Kintner C, Rubin GM (2001) *Drosophila* neuralized is a ubiquitin ligase that promotes the internalization and degradation of delta. *Dev Cell* 1: 783 – 794

Liu J, Stevens J, Rote CA, Yost HJ, Hu Y, Neufeld KL, White RL, Matsunami N (2001) Siah-1 mediates a novel β-catenin degradation pathway linking p53 to the adenomatous polyposis coli protein. *Mol Cell* 7: 927 – 936

Liu X, Fu J, Bi H, Ge A, Xia T, Liu Y, Sun H, Li D, Zhao Y (2019) DNA methylation of SFRP1, SFRP2, and WIF1 and prognosis of postoperative colorectal cancer patients. *BMC Cancer* 19: 1212

MacDonald BT, Tamai K, He X (2009) Wnt/β-catenin signaling: components, mechanisms, and diseases. *Dev Cell* 17: 9 – 26

Meijer L, Skaltsounis A-L, Magiatis P, Polychronopoulos P, Knockaert M, Leost M, Ryan XP, Vonica CA, Brivanlou A, Dajani R *et al* (2003) GSK-3-selective inhibitors derived from Tyrian purple indirubins. *Chem Biol* 10: 1255 – 1266

Nakamura H, Yoshida M, Tsuiki H, Ito K, Ueno M, Nakao M, Oka K, Tada M, Kochi M, Kuratsu J *et al* (1998) Identification of a human homolog of the *Drosophila* neuralized gene within the 10q25.1 malignant astrocytoma deletion region. *Oncogene* 16: 1009 – 1019

Nastasi T, Bongiovanni A, Campos Y, Mann L, Toy JN, Bostrom J, Rottier R, Hahn C, Conaway JW, Harris AJ *et al* (2004) Ozz-E3, a muscle-specific ubiquitin ligase, regulates β-catenin degradation during myogenesis. *Dev Cell* 6: 269 – 282

Nusse R, Clevers H (2017) Wnt/β-catenin signaling, disease, and emerging therapeutic modalities. *Cell* 169: 985 – 999

Ou C-Y, LaBonte MJ, Manegold PC, So AY-L, Ianculescu I, Gerke DS, Yamamoto KR, Ladner RD, Kahn M, Kim JH *et al* (2011) A coactivator role of CARM1 in the dysregulation of β-catenin activity in colorectal cancer cell growth and gene expression. *Mol Cancer Res* 9: 660 – 670

Park J-M, Choi JY, Yi JM, Chung JW, Leem S-H, Koh SS, Kang T-H (2015) NDR1 modulates the UV-induced DNA-damage checkpoint and nucleotide excision repair. *Biochem Biophys Res Commun* 461: 543 – 548

Pavlopoulos E, Pitsouli C, Klueg KM, Muskavitch MAT, Moschonas NK, Delidakis C (2001) Neuralized encodes a peripheral membrane protein involved in delta signaling and endocytosis. *Dev Cell* 1: 807 – 816

Ruan Y, Tecott L, Jiang M-M, Jan LY, Jan YN (2001) Ethanol hypersensitivity and olfactory discrimination defect in mice lacking a homolog of *Drosophila* neuralized. *Proc Natl Acad Sci USA* 98: 9907 – 9912

Schuebel KE, Chen W, Cope L, Glöckner SC, Suzuki H, Yi JM, Chan TA, Neste LV, Criekinge WV, Bosch SV *et al* (2007) Comparing the DNA hypermethylome with gene mutations in human colorectal cancer. *PLoS Genet* 3: 1709 – 1723

Sharma M, Molehin D, Castro-Piedras I, Martinez EG, Pruitt K (2019) Acetylation of conserved DVL-1 lysines regulates its nuclear translocation and binding to gene promoters in triple-negative breast cancer. *Sci Rep* 9: 16257

Suzuki H, Gabrielson E, Chen W, Anbazhagan R, van Engeland M, Weijenberg MP, Herman JG, Baylin SB (2002) A genomic screen for genes upregulated by demethylation and histone deacetylase inhibition in human colorectal cancer. *Nat Genet* 31: 141 – 149

Suzuki H, Watkins DN, Jair KW, Schuebel KE, Markowitz SD, Chen WD, Pretlow TP, Yang B, Akiyama Y, Van Engeland M *et al* (2004) Epigenetic inactivation of SFRP genes allows constitutive WNT signaling in colorectal cancer. *Nat Genet* 36: 417 – 422

Tetsu O, McCormick F (1999) [beta]-Catenin regulates expression of cyclin D1 in colon carcinoma cells. *Nature* 398: 422 – 426

Timmusk T, Palm K, Belluardo N, Mudò G, Neuman T (2002) Dendritic localization of mammalian neuralized mRNA encoding a protein with transcription repression activities. *Mol Cell Neurosci* 20: 649 – 668

Vollrath B, Pudney J, Asa S, Leder P, Fitzgerald K (2001) Isolation of a murine homologue of the *Drosophila* neuralized gene, a gene required for axonemal integrity in spermatozoa and terminal maturation of the mammary gland. *Mol Cell Biol* 21: 7481 – 7494

Xue J, Chen Y, Wu Y, Wang Z, Zhou A, Zhang S, Lin K, Aldape K, Majumder S, Lu Z *et al* (2015) Tumour suppressor TRIM33 targets nuclear β-catenin degradation. *Nat Commun* 6: 6156

Yamamoto E, Suzuki H, Yamano H-O, Maruyama R, Nojima M, Kamimae S, Sawada T, Ashida M, Yoshikawa K, Kimura T *et al* (2012) Molecular dissection of premalignant colorectal lesions reveals early onset of the CpG island methylator phenotype. *Am J Pathol* 181: 1847 – 1861

Yeh E, Zhou L, Rudzik N, Boulianne GL (2000) Neuralized functions cell autonomously to regulate *Drosophila* sense organ development. *EMBO J* 19: 4827 – 4837

Yeh E, Dermer M, Commisso C, Zhou L, McGlade CJ, Boulianne GL (2001) Neuralized functions as an E3 ubiquitin ligase during *Drosophila* development. *Curr Biol* 11: 1675 – 1679

Yi JM, Dhir M, Van Neste L, Downing SR, Jeschke J, Glöckner SC, de Freitas Calmon M, Hooker CM, Funes JM, Boshoff C *et al* (2011) Genomic and epigenomic integration identifies a prognostic signature in colon cancer. *Clin Cancer Res* 17: 1535 – 1545

Yu F, Yu C, Li F, Zuo Y, Wang Y, Yao L, Wu C, Wang C, Ye L (2021) Wnt/β-catenin signaling in cancers and targeted therapies. *Signal Transduct Target Ther* 6: 307

